Talanta 116 (2013) 575–580

Contents lists available at ScienceDirect

Talanta

journal homepage: www.elsevier.com/locate/talanta

Direct separation of faradaic and double layer charging current in potential step voltammetry

Jiarun Tu, Wensheng Cai, Xueguang Shao*

State Key Laboratory of Medicinal Chemical Biology, and Research Center for Analytical Sciences, College of Chemistry, Nankai University, Tianjin 300071, People's Republic of China

ARTICLE INFO

Article history:
Received 6 May 2013
Received in revised form
2 July 2013
Accepted 9 July 2013
Available online 24 July 2013

Keywords:
Capacitance current
Faradaic current
ITTFA
NPV
Potential step

ABSTRACT

Double layer charging current in electrochemical systems has been a challenging problem in the last several decades because it causes interference to the accurate measurement of faradaic current. A method for extracting faradaic current and double layer charging current directly from the measured total current in potential step voltammetry is developed by using iterative target transformation factor analysis (ITTFA). The method constructs initial target vectors based on the theoretical formulae of faradaic and charging current, and then calculates the weights of faradaic and charging current in the measured signal via the iterative transformation of the initial vectors. Therefore, the two currents in one experiment can be obtained simultaneously without any assumption. The potential step voltammetric signals of potassium ferricyanide, copper sulfate and paracetamol were analyzed with the proposed method. The results show that the shape of the obtained voltammogram is an ideal sigmoid curve with horizontal straight baseline and plateaus, and the intensity of the signal is greatly enhanced. Therefore, the method provides a new way to measure the pure faradic current in the potential step voltammetric experiment, and may provide an alternative for improving the sensitivity of quantitative analysis.

1. Introduction

How to separate faradaic current from double layer charging current in an electrochemical system that has been a challenge in the last several decades [1–3]. Double layer charging current, which is generated with the change of potential on the working electrode surface, causes interference to faradaic current and restricts the detection limit and accuracy of the measurement [4]. Most of the work has been focused on minimizing the contribution of charging current to total current signal [5,6]. Many efforts have been made to improve the experimental instrument or signal pattern for increasing faradaic to charging current ratio, such as circuitry design [7], duplicate electrolysis cells [8,9], microelectrode [10,11], sinusoidal voltammetry and staircase voltammetry [12–15], etc. However, the difference between reference and sample, and the difficulty of parameter selection may lead to incorrect or incomplete elimination of charging current.

Chemometrics has speeded up the development of electrochemical analysis [16–23]. With the aid of chemometric methods, such as curve-fitting [24,25], Kalman filter [26], derivative techniques [27], Fourier transform [28–31], mathematical processing techniques for improving the faradaic to charging current ratio becomes viable. Based on the differences between faradaic and charging current, interference of charging current can be eliminated by means of mathematical processing. However, it is still difficult to clearly know the absolute values and variation trend of charging current in an electrochemistry system. Besides, there have been methods for separating faradaic current from charging current with the assumptions of electrode process, such as the method based on electrochemical impedance spectroscopy [32], a posteriori or a priori separation [33–36]. These methods are based on certain assumptions and need to simultaneously determine several proper circuit or experimental parameters. Nevertheless, it is not an easy task to determine the accurate value of the parameters. The number of the parameters can be reduced if additional assumptions about the double layer model are introduced. This, however, makes the problem more complex.

In this paper, a method is presented to directly separate faradaic current from double layer charging current in potential step voltammetry via iterative target transformation factor analysis (ITTFA). ITTFA has been successfully applied in determination of a specific component in mixtures by means of an iterative transformation of a target vector representing the character of the component [37,38]. The core idea of the method is to iteratively transform the initial target vector to obtain the weight (concentration) of the component in an overlapping signal. In this study, the initial target vectors are constructed based on faradaic or charging decaying current formula, and then the weight of the faradaic and double layer charging current can be calculated with

* Corresponding author. Tel.: +86 22 23503430; fax: +86 22 23502458.
E-mail address: xshao@nankai.edu.cn (X. Shao).

0039-9140/$ - see front matter © 2013 Elsevier B.V. All rights reserved.
http://dx.doi.org/10.1016/j.talanta.2013.07.021

the iterative transofrmation. Therefore, the approach can simultaneously obtain the faradaic and charging current, respectively, from the measured current in one experiment without any assumption.

2. Experimental

2.1. Chemical reagents

All chemical reagents used were of analytical grade except paracetamol of chemical grade. A further purification will be better for obtaining more precise measurements; these reagents were directly used to make the proposed method more practical. Potassium ferricyanide (99.5%), potassium nitrate (99%), copper sulfate (99%), anhydrous sodium sulfate (99%), paracetamol (98%) and hydrochloric acid were purchased from Guangfu Chemical Co., Ltd. (Tianjin, China). Potassium ferricyanide, copper sulfate and paracetamol solutions were prepared with 0.5 M potassium nitrate, 0.1 M sodium sulfate and 0.2 M hydrochloric acid, respectively. Doubly distilled water was used in preparation of the samples.

2.2. Instrumentation and procedures

A self-made electrochemical workstation was used, consisting of a data acquisition card (NI USB-6211, National Instruments Corporation, Texas, USA), potentiostat circuit board (Lanlike Chemistry & Electron High Technology Co., Ltd., Tianjin, China) and personal computer (Lenovo, Beijing, China). The programs were written in MATLAB (The MathWorks Inc., USA). Three electrode system made up of a 3 mm-diameter bare glassy carbon electrode (working electrode), a saturated calomel electrode (reference electrode) and a platinum sheet electrode (auxiliary electrode) was used for all the measurements. All potentials reported were referred to the saturated calomel electrode (SCE). Different electrode systems can be used for investigation of the proposed method, the commonly used electrode system, however, was used for generalization.

In the potential step experiments, normal pulse voltammetry was used, i.e., the potential form is consisted of a series of pulses, and each pulse increases to a potential and returns to the initial value. A pulse width of 60 ms and interval of 1.0 s between successive pulses were employed. Sampling rate is 20,000 points per second. For potassium ferricyanide, the potential was scanned in the range from 0.6 to -0.2 V with an increment of -0.02 V. For copper sulfate and paracetamol, the potential ranges 0.4 to -0.4 V and 1.1 to 0.3 V, increased by -0.02 V, were used. All solutions were carefully degassed with high-purity nitrogen for 5 min prior to the measurements in order to remove oxygen. All the experiments were carried out at room temperature (ca. 25 °C).

3. Theory and calculations

3.1. Basic idea

In potential step voltammetry, the measured current is a total of faradaic and charging current. The former decays in accordance with squared root of time, while the latter decays exponentially with time. The separation of the two currents can be realized based on the different decaying rates. The idea of the proposed method is to construct the initial target vectors based on the theoretical formula of the two currents and then to calculate the weights of them in the measured signal. Finally the two currents in an electrochemical system can be obtained by multiplying the final target vector and the loading (weights) vector. Therefore, the approach can simultaneously calculate the faradaic current and charging current, respectively, from the measured current data in one experiment without any assumption.

3.2. Iterative target transformation factor analysis (ITTFA)

The basic model for an analytical signal of multicomponent system can be written as,

$$\mathbf{D} = \mathbf{S}\mathbf{C}^T \tag{1}$$

where **D** denotes the measured signal, **S** represents the pure or standard signal of the components and **C** means the concentration (relative to the standards) of the components. In this study, **S** is composed of two vectors representing the faradic and changing current, respectively, and **C** means the relative weights of the two currents in the measured total current. The superscript T means the transposition operation.

The aim of ITTFA is to calculate **S** and **C** from a measured **D** with an initial target vector constructed with estimations of the components. To achieve the purpose, principal component analysis (PCA) can be performed to obtain a score matrix **R**, a loading matrix **V**, and the eigenvalues λ of the matrix **D**.

$$\mathbf{D} = \mathbf{R}\mathbf{V}^T \tag{2}$$

Mathematically, the vectors in loading matrix are combinations of the vectors in **C**, and the score matrix corresponds to the weights of the combination. Therefore, **R** and **V** can be converted to **S** and **C** by mathematical transformation. If a target vector $\overline{\mathbf{R}}_l$ is provided, a transformation matrix or projection matrix $\mathbf{T}_l$ can be obtained to transform **R** to **S**.

$$\mathbf{T}_l = \lambda^{-1}\mathbf{R}^T\overline{\mathbf{R}}_l \tag{3}$$

$$\mathbf{S}_l = \mathbf{R}\mathbf{T}_l = \mathbf{R}\lambda^{-1}\mathbf{R}^T\overline{\mathbf{R}_l} \tag{4}$$

Defining $\mathbf{P} = \mathbf{R}\lambda^{-1}\mathbf{R}^T$

$$\mathbf{S}_l = \mathbf{P}\overline{\mathbf{R}}_l \tag{5}$$

Furthermore, when the values in $\overline{\mathbf{R}}_l$ are not exactly correct, corrections of these values can be obtained by iteratively replacing the values in $\overline{\mathbf{R}}_l$ with the values in the calculated $\mathbf{S}_l$. Therefore, the calculation of ITTFA can be summarized as [38],

(1). Perform PCA to the data matrix **D**, obtaining **R** and λ.
(2). Construct an initial iterative target vector $\overline{\mathbf{R}}_l$, and calculate $\mathbf{T}_l$ and **P** matrix using Eqs. (3) and (4).
(3). Calculate $\mathbf{S}_l$ using Eq. (5) iteratively by replaceing $\overline{\mathbf{R}}_l$ by $\mathbf{S}_l$ until $\overline{\mathbf{R}}_l$ does not change.

3.3. Direct separation of faradic and charging current by ITTFA

The idea of the proposed method is to construct the initial target vectors using faradaic or charging current formula and then to achieve the separation using ITTFA. The following steps are included in the calculations:

(1). Prepare the decaying current matrix (**D**): The decaying current of each potential step is measured and the matrix $\mathbf{D}_{n\times m}$ is constructed by aligning the decaying current at each pulse, where n denotes the data point number sampled in a pulse and m denotes the number of pulses at different potentials.
(2). Construct the initial iterative target vectors using Eqs. (6) and (7), respectively.

$$i_f = f(E)t^{-1/2} \tag{6}$$

$$i_c = \frac{\Delta E}{R_\Omega}\exp\left(\frac{-t}{\tau}\right) \quad (7)$$

where i_f is faradaic current, i_c is double layer charging current, ΔE is the potential step, R_Ω is the uncompensated cell resistance, t is the duration time from the beginning of the pulse, τ is the cell time constant (50 μs [39] was used), and $f(E)$ is a function related to the step potential,

$$f(E) = \frac{nFAD_{ox}^{1/2}C_{ox}^{*}}{\pi^{1/2}}\left[1+\exp\left(\frac{nF}{RT(E-E_{1/2})}\right)\right]^{-1} \quad (8)$$

where n is number of electrons exchanged per molecule, F is Faraday constant, A is the area of the electrode, D_{ox} is the diffusion coefficient of the oxidized species, C_{ox}^{*} is the concentration of the oxidized species, R is ideal gas constant (8.314 J mol^{-1} K^{-1}), T is Kelvin temperature (298.15 K), E is the potential of working electrode, and $E_{1/2}$ is the half-wave potential.

To construct proper initial iterative target vectors ($\overline{\mathbf{R}}_l$) of faradaic and charging current, t is set from 0 to 60 ms with the same interval used in the experiment. It should be noted that modifications to the vectors generated with the theoretical formula is needed because the currents do not comply with the theory during all the pulse time. In the single potential step experiment, the total current and the charging current decay continuously with time during the experiment, while the faradaic current increases at first, reaches a maximum about the time of one cell time constant (50 μs), and then decays with time [39]. Therefore, the initial iterative target vector for the charging current was generated directly by its theoretical formula during the entire pulse time, but zeros were used in the initial iterative target vector for the faradaic current before one cell time constant. The zeros are not correct but the correct values can be obtained after the iterations. Furthermore, in the construction of the initial target vectors, $f(E)$ and $\frac{\Delta E}{R_\Omega}$ were set to 1. Therefore, a correction step must be adopted after the calculation.

(3). ITTFA. Using the constructed initial vectors ($\overline{\mathbf{R}}_l$), two vectors of $\mathbf{S}_l$ can be obtained, corresponding to the faradaic and charging current, respectively.

(4). Calculate the weighting curves $\mathbf{C}_r$ according to Eq. (9).

$$\mathbf{C}_r^T = (\mathbf{S}_l^T\mathbf{S}_l)^{-1}\mathbf{S}_l^T\mathbf{D} \quad (9)$$

(5). Calculate the faradaic and charging current ($\mathbf{i}_l$) using Eq. (10).

$$\mathrm{i}_l = \mathrm{S}_l\mathrm{C}_r^T \quad (10)$$

3.4. Calibration of the calculated faradaic current weighting curve

Because $f(E)=1$ was used in the construction of the initial target vector for the faradaic current, the weighting curve must be calibrated to obtain the voltammogram. According to Eq. (8), the calibration factor matrix $\mathbf{K}=f(\boldsymbol{E})$ can be obtained using the parameters of the analyzing system. Then, the corrected weighting curve $\mathbf{C}_{fr}$, i.e., the normal pulse voltammogram, can be obtained by

$$\mathbf{C}_{fr} = \mathbf{C}_r\sqrt{\mathbf{K}\mathbf{K}^T} \quad (11)$$

4. Results and discussion

4.1. Separation of the faradaic and charging current

To evaluate the performance of the method, the current signals of potassium ferricyanide in aqueous potassium nitrate electrolyte in a set of different step potentials (pulses) were adopted. Aligning the decaying current in each pulse (as shown in Fig. 1a) forms a current matrix $\mathbf{D}_{n\times m}$, where n denotes the data point number sampled in a pulse and m denotes the number of pulses. Then the score matrix $\mathbf{R}$, loading matrix $\mathbf{V}$ and the eigenvalue λ can be obtained by performing singular value decomposition (SVD) to the matrix $\mathbf{D}$. The result of the eigenvalue shows that the two larger ones explain more than 99% of the information in the data matrix. This indicates that only two kinds of currents, i.e., faradaic current and charging current, exist in the matrix $\mathbf{D}$. Hence, the projection matrix $\mathbf{P}$ in Eq. (5) can be obtained with two principal components. With the projection matrix, faradaic current and double layer charging current can be extracted from the experimental signal by ITTFA with the initial iterative target vectors, respectively. The results are shown in Fig. 1b. It can be seen that the faradaic current increases very fast to a maximum and then decays with time, while the charging current decays in a more rapid way. Before around 3 ms, the charging current plays a predominant role in the total current, while the faradaic current becomes dominant gradually with time. The results are obviously consistent with the previous works [39].

The red curve in Fig. 1c shows the variation of the calculated weights of the faradaic current with the pulse potential. It is not a correct normal pulse voltammogram because the same initial iterative target vector was used in resolving the data matrix at different pulse potentials. Therefore, a correction is needed to adjust the potential influence on faradaic current. After the correction using Eq. (11), the blue curve in Fig. 1c can be obtained. The weighting curve is obviously a standard sigmoid curve with horizontal straight baseline and plateaus, corresponding to an ideal normal pulse voltammogram.

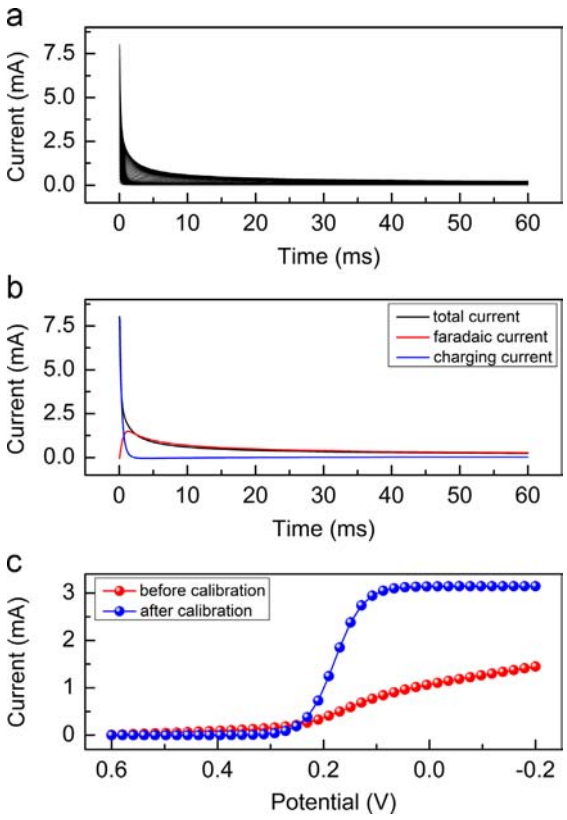

Fig. 1. Experiment data and resolved results. (a) Experimental decaying total current of each potential step for 0.5 mM potassium ferricyanide solution. (b) Faradaic current (red) and double layer charging current (blue) resolved by ITTFA compared with the total current (black) under a pulse. (c) Weighting curves before (red) and after (blue) calibration for different step potentials. (For interpretation of the references to color in this figure legend, the reader is referred to the web version of this article.)

4.2. Quantitative determination

Generally, two approaches can be used for quantitative analysis. One is based on the proportional relationship of electric quantity and concentration. Integrating the resolved faradaic current in the pulse time (the red curve in Fig. 1b), the electric quantity can be obtained and used to calculate the concentration of the sample. Alternatively, there is a proportional relationship between the peak height in a voltammogram and concentration. The peak height of the blue curve in Fig. 1c can be measured and used to estimate the concentration of the sample. The difficulty for both the approaches comes from the interference of the charging current in the conventional normal pulse voltammetric method. In the proposed method, however, the calculation becomes very easy because both the curves in Fig. 1b and c are composed of pure faradaic current.

To validate the practicability of the proposed method, a series of potassium ferricyanide solution with different concentrations from 0.2 mM to 10.0 mM was prepared and measured with different pulse potentials from 0.6 V to −0.2 V. The comparatively high concentration samples were used to make the experiment results comply well with the theoretical equations of faradaic and charging current. With ITTFA, faradaic and double layer charging current of each sample can be obtained, respectively. As shown in Fig. 2, the faradaic current increases with potassium ferricyanide concentration. This may be a proof of correct separation of the two currents, because the faradaic current is highly related to the concentration. As mentioned above, the electric quantity can be obtained by integrating the faradaic current along the pulse time and the quantity is proportional to the concentration. The figure in the top-right corner of Fig. 2 shows the relationship between the quantity and concentration. As shown in the figure, an excellent correlation coefficient (0.9995) was obtained, demonstrating that

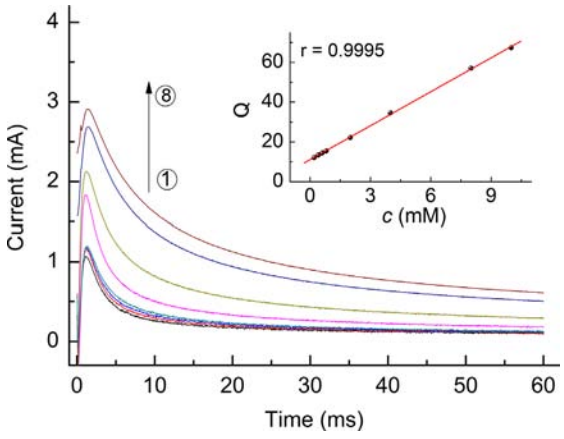

Fig. 2. Faradaic current separated from the measured voltammograms of different concentrations of potassium ferricyanide in 0.5 M aqueous potassium nitrate electrolyte at the pulse potential −0.2 V. Concentrations: ① 0.2 mM; ② 0.4 mM; ③ 0.6 mM; ④ 0.8 mM; ⑤ 2.0 mM; ⑥ 4.0 mM; ⑦ 8.0 mM; and ⑧ 10.0 mM. Quantitative relationship between electric quantity and concentration is displayed in the top-right corner.

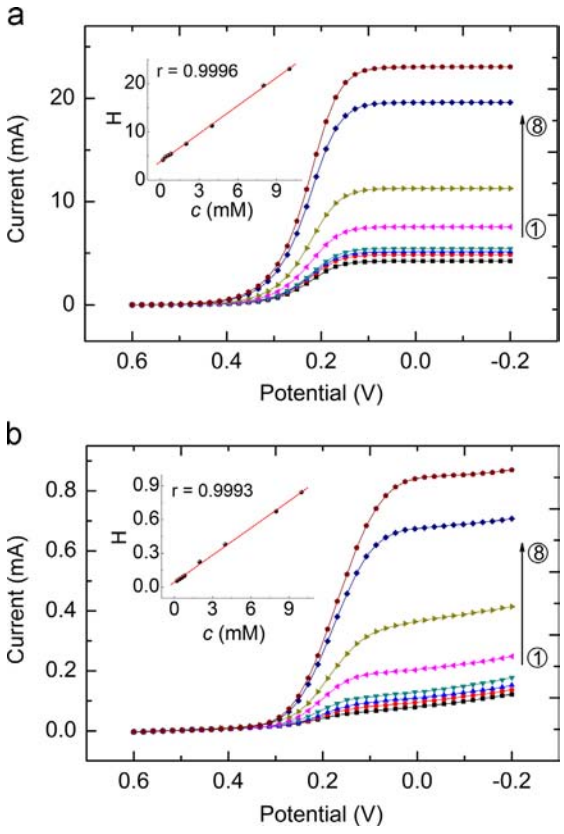

Fig. 3. Voltammograms of different concentrations of potassium ferricyanide in 0.5 M potassium nitrate. Concentrations: ① 0.2 mM; ② 0.4 mM; ③ 0.6 mM; ④ 0.8 mM; ⑤ 2.0 mM; ⑥ 4.0 mM; ⑦ 8.0 mM; and ⑧ 10.0 mM. (a) Voltammograms calculated by ITTFA. (b) Voltammograms recorded by conventional method. The current is sampled at 20 ms. The relationship between the peak height and concentration is displayed in the top-left corner of the two figures, respectively.

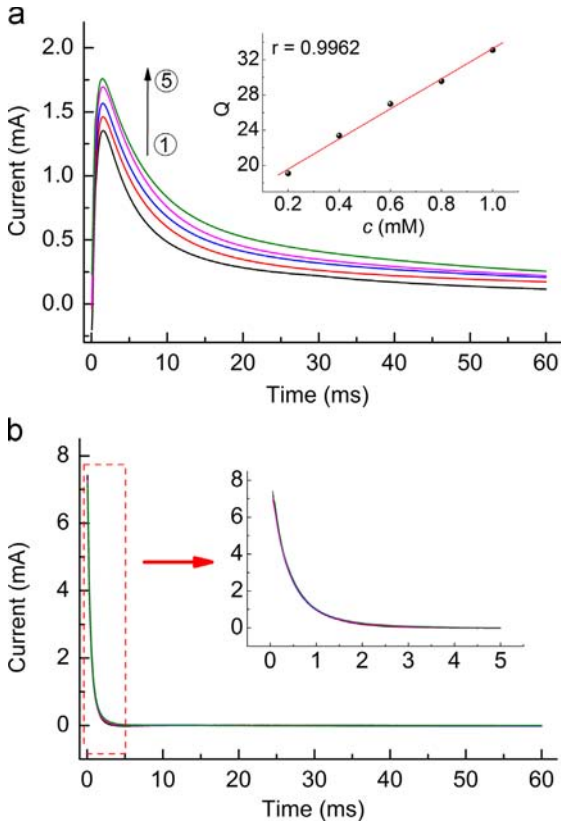

Fig. 4. Faradaic current and double layer charging current of different concentrations of copper sulfate in 0.1 M aqueous sodium sulfate electrolyte at the pulse potential −0.4 V. Concentrations: ① 0.2 mM; ② 0.4 mM; ③ 0.6 mM; ④ 0.8 mM; and ⑤ 1.0 mM. (a) Faradaic current. From the bottom up, faradaic current increases with concentrations. Quantitative result of electric quantity and concentration is displayed in the top-right corner. (b) Charging current. Charging current rapidly decays to 0 and almost does not change with the concentration. The top-right figure shows the enlarged part before 5 ms pulse time.

quantitative analysis can be achieved from the separated faradaic current. This may be another proof of the perfect separation.

The voltammogram shown in Fig. 1c is more frequently used for quantitative analysis. Therefore, the calibrated weighting curves obtained from the samples of different concentrations are calculated. As shown in Fig. 3a, each curve is an ideal normal pulse voltammogram and the peak height increases with the concentration. The top-left figure shows the relationship of the peak heights and concentrations. A perfect straight line with a correlation coefficient 0.9996 is obtained by least square fitting of these points, proving again the reliability of the method for quantitative analysis.

As a comparison, the voltammograms obtained with conventional method were measured and shown in Fig. 3b. In the experiments, the current is sampled at 20 ms of the pulse. The relationship of the peak height and concentration is displayed in the top-left corner of the figure. Comparing the two figures of Fig. 3a and b, two advantages can be found for the new method. At first, the voltammograms obtained by the calculation are ideal sigmoid curves with horizontal straight baseline and plateaus, which makes measurement of peak height easier. More importantly, the scale of the current axis is increased about 20 times, implying that the sensitivity of the quantitative analysis is greatly improved. The increase can be explained by the fact that the current in conventional method is recorded at 20 ms after the pulse, but current in the proposed method is a measure of the maximal peak in the whole duration of the pulse as shown in Figs. 1b and 2.

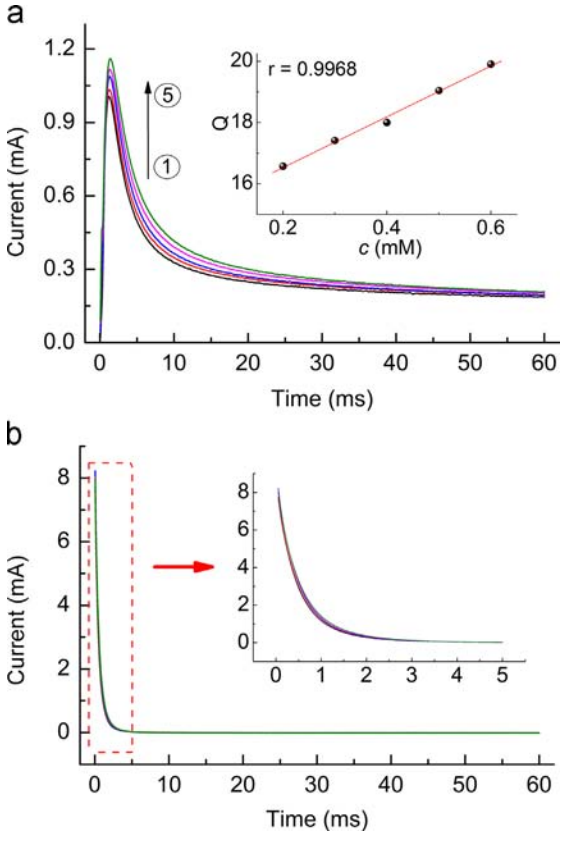

Fig. 5. Faradaic current and double layer charging current of different concentrations of paracetamol in 0.2 M hydrochloric acid electrolyte solution at the pulse potential 0.3 V. Concentrations: ① 0.2 mM; ② 0.3 mM; ③ 0.4 mM; ④ 0.5 mM; and ⑤ 0.6 mM. (a) Faradaic current. From the bottom up, faradaic current increases with concentrations. Quantitative result of electric quantity and concentration is displayed in the top-right corner. (b) Charging current. Charging current rapidly decays to 0 and almost does not change with the concentration. The top-right figure shows the enlarged part before 5 ms pulse time.

4.3. Further validation

To further validate the practicability of the proposed method, non-reversible redox system was investigated. A set of copper sulfate solutions in 0.1 M sodium sulfate electrolyte with concentration from 0.2 mM to 1.0 mM and a set of paracetamol solutions in 0.2 M hydrochloric acid electrolyte solution with concentration from 0.2 mM to 0.6 mM were prepared and measured under the same conditions. Figs. 4 and 5 show the extracted faradaic and charging current by ITTFA. The similar results as potassium ferricyanide can be found in the two figures. Fig. 6a and b shows the voltammograms obtained by ITTFA calculations. Clearly, all the two voltammograms are as perfect as that for potassium ferricyanide, and the correlation coefficients for calibration curves in the top-left figures are as high as 0.9995 and 0.9968, respectively. Therefore, direct separation of faradaic current and double layer charging current in potential step voltammetry by ITTFA should be feasible as a universal approach for different redox systems.

5. Conclusion

A method for direct separation of faradaic current and the double layer charging current in potential step voltammetry using ITTFA is proposed. The approach achieves the currents separation through iterative transformation of the initial target vectors constructed with the theoretical formula of faradaic and charging current. The results show that the two currents can be completely separated from one experiment without any assumption, and ideal

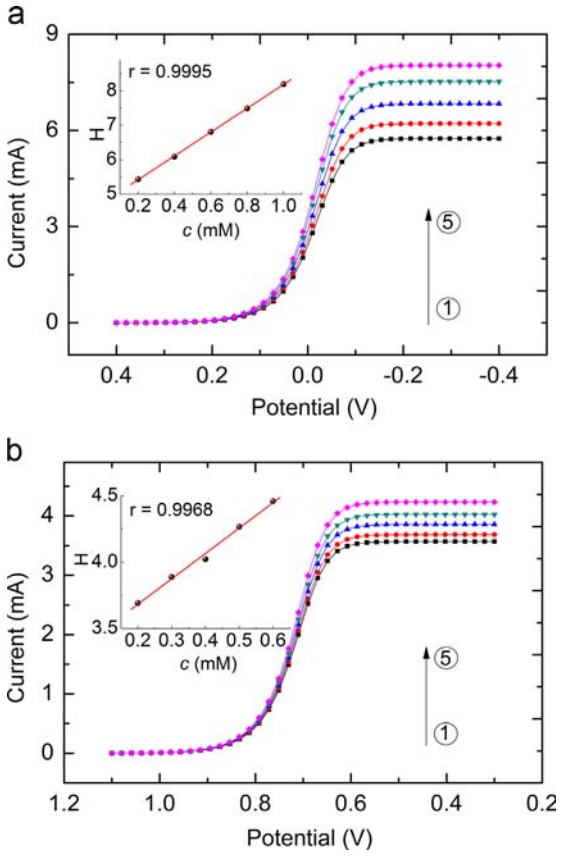

Fig. 6. Voltammograms of different concentrations of copper sulfate and paracetamol. (a) copper sulfate in 0.1 M sodium sulfate. Concentrations: ① 0.2 mM; ② 0.4 mM; ③ 0.6 mM; ④ 0.8 mM; and ⑤ 1.0 mM. (b) Paracetamol in 0.2 M hydrochloric acid electrolyte solution. Concentrations: ① 0.2 mM; ② 0.3 mM; ③ 0.4 mM; ④ 0.5 mM; and ⑤ 0.6 mM. The relationship between the peak height and concentration is displayed in the top-left corner of the two figures, respectively.

voltammograms can be obtained because they are composed of pure faradaic current. The calibration curves of the electric quantity and peak height in the voltammograms versus concentration can further prove the reliability of the separation. Furthermore, in contrast to the conventional method that records the current at 20 ms delay of the pulse for avoiding the charging current, the proposed method provides a measure of the faradaic current in the whole duration of the pulse. Therefore, the sensitivity of the quantitative analysis may be improved. More importantly, the method obtains the faradaic and charging current in one experiment, the charging current, therefore, is a real reflection of the system. This may offer helps to study the electrode process for electrochemical systems.

Acknowledgments

This work was supported by National Natural Science Foundation of China (No. 21175074).

References

[1] M.R. Wasielewski, R. Breslow, J. Am. Chem. Soc. 98 (1976) 4222–4229.
[2] R.M. Wightman, D.O. Wipf, Acc. Chem. Res. 23 (1990) 64–70.
[3] A. Hermans, R.B. Keithley, J.M. Kita, L.A. Sombers, R.M. Wightman, Anal. Chem. 80 (2008) 4040–4048.
[4] M.C. Weston, M.D. Gerner, I. Fritsch, Anal. Chem. 82 (2010) 3411–3418.
[5] R.B. Keithley, P. Takmakov, E.S. Bucher, A.M. Belle, C.A. Owesson-White, J. Park, R.M. Wightman, Anal. Chem. 83 (2011) 3563–3571.
[6] A.G. Ewing, M.A. Dayton, R.M. Wightman, Anal. Chem. 53 (1981) 1842–1847.
[7] L.H. Chow, G.W. Ewing, Anal. Chem. 51 (1979) 322–327.
[8] W.D. Shults, F.E. Haga, T.R. Mueller, H.C. Jones, Anal. Chem. 37 (1965) 1415–1416.
[9] P. Bos, E. Van Dalen, J. Electroanal. Chem. Interfacial Electrochem. 45 (1973) 165–179.
[10] R.M. Wightman, Anal. Chem. 53 (1981) 1125A–1134A.
[11] K. Stulík, C. Amatore, K. Holub, V. Marecek, W. Kutner, Pure Appl. Chem. 72 (2000) 1483–1492.
[12] P. Singhal, W.G. Kuhr, Anal. Chem. 69 (1997) 3552–3557.
[13] P. Singhal, K.T. Kawagoe, C.N. Christian, W.G. Kuhr, Anal. Chem. 69 (1997) 1662–1668.
[14] R. Bilewicz, R.A. Osteryoung, J. Osteryoung, Anal. Chem. 58 (1986) 2761–2765.
[15] J.H. Christie, P.J. Lingane, J. Electroanal. Chem. 10 (1965) 176–182.
[16] M. Esteban, C. Ariño, J.M. Díaz-Cruz, TrAC Trends in Anal. Chem. 25 (2006) 86–92.
[17] Y.N. Ni, S. Kokot, Anal. Chim. Acta 626 (2008) 130–146.
[18] J.M. Palacios-Santander, L.M. Cubillana-Aguilera, I. Naranjo-Rodríguez, J. L. Hidalgo-Hidalgo-de-Cisneros, Chemom. Intell. Lab. Syst. 85 (2007) 131–139.
[19] M.R. Moghadam, S. Dadfarnia, A.M. Shabani, P. Shahbazikhah, Anal. Biochem. 410 (2011) 289–295.
[20] Y.N. Ni, L. Wang, S. Kokot, Anal. Chim. Acta 439 (2001) 159–168.
[21] M.J. López, C. Ariño, S. Díaz-Cruz, J.M. Díaz-Cruz, R. Tauler, M. Esteban, Environ. Sci. Technol. 37 (2003) 5609–5616.
[22] M.C. Antunes, J.E. Simão, A.C. Duarte, Electroanal. 13 (2001) 1041–1045.
[23] X.Q. Lin, Z.H. Chen, X.G Shao, Z.X Deng, Chin. J. Anal. Chem. 27 (1999) 1381–1385.
[24] C. Montella, J. Electroanal. Chem. 518 (2002) 61–83.
[25] J.W. Dillard, K.W. Hanck, Anal. Chem. 48 (1976) 218–222.
[26] M. Bos, Talanta 33 (1986) 583–586.
[27] A. Bond, B. Grabaric, Anal. Chim. Acta 101 (1978) 309–318.
[28] J. Zhang, S.X. Guo, A.M. Bond, F. Marken, Anal. Chem. 76 (2004) 3619–3629.
[29] S. Guo, J. Zhang, D.M. Elton, A.M. Bond, Anal. Chem. 76 (2004) 166–177.
[30] S.M. Matthews, M.J. Shiddiky, K. Yunus, D.M. Elton, N.W. Duffy, Y. Gu, A. C. Fisher, A.M. Bond, Anal. Chem. 84 (2012) 6686–6692.
[31] Z.H. Chen, X.Q. Lin, X.G. Shao, Z.X. Deng, Chin. J. Anal. Chem. 29 (2001) 625–628.
[32] B. Ulgut, J.E. Grose, Y. Kiya, D.C. Ralph, H.D. Abruña, Appl. Surf. Sci. 256 (2009) 1304–1308.
[33] K. Holub, G. Tessari, P. Delahay, J. Phys. Chem. 71 (1967) 2612–2618.
[34] P. Delahay, G.G. Susbielles, J. Phys. Chem. 70 (1966) 3150–3157.
[35] K. Nisancioglu, J. Newman, J. Electrochem. Soc. 159 (2012) E59–E61.
[36] J.N. Butler, M.L. Meehan, J. Phys. Chem. 69 (1965) 4051–4052.
[37] U. Evans, O. Soyemi, M.S. Doescher, U.H.F. Bunz, L. Kloppenburg, M.L. Myrick, Analyst 126 (2001) 508–512.
[38] Z.L. Zhu, W.Z. Cheng, Y. Zhao, Chemom. Intell. Lab. Syst. 64 (2002) 157–167.
[39] L.H.L. Miaw, S.P. Perone, Anal. Chem. 51 (1979) 1645–1650.